

# **Control of streak structures in wall turbulence using a piezo-ceramic actuator array**

Takehiko Segawa, Yasuo Kawaguchi, Yoshihiro Kikushima,  
Hiroyuki Abe, Takayuki Matsunuma and Hiro Yoshida

*Mechanical Engineering Laboratory, AIST, METI, Japan*

In turbulent channel flows, spanwise wall oscillation is known to considerably reduce frictional drag. In this study, turbulent flow control using an actuator array and related modification of the turbulent spatial structure were experimentally examined using a PIV system. The actuator array can create spanwise fluctuations in the flow in the vicinity of the wall by changing the mode of actuator elements and decreasing the regularity of streak-like structures.

## **1. INTRODUCTION**

The control of turbulent flows using a micro electro-mechanical system (MEMS) is one of the most challenging recent topics in fluid engineering. In this study we tried to clarify 3-dimensional flow structures at the near-wall region when they are stimulated by artificial disturbances. In the past turbulent flows were believed to be completely random. However, a sort of coherent structure was found in the turbulent boundary layers (Hama, et al. 1957, Kline, et al. 1967). This discovery indicated the possibility of controlling turbulence with respect to the coherent motion. Recent development in flow visualization techniques using laser technology enables us to observe perspective views of the coherent structures in the wall turbulence, such as horseshoe vortices or stream-wise vortices. Moreover, recent studies have provided hopeful results for controlling turbulence. For example, Choi, et al. (1994) indicated numerically that drag in a turbulent channel flow could be decreased 30% if local blowing/suction on the wall was properly arranged and controlled. Using MEMS devices, Stuart, et al. (1998) demonstrated in experiments that Reynolds stresses could be in fact regulated to a certain degree.

Although active control technologies using actuator devices are under development, few examples of turbulent drag reduction by active boundaries have been reported. In turbulent channel flows, spanwise wall oscillation is known to generate considerable reduction of the drag. Jung et al. (1992) used numerical simulation to show the effect of spanwise oscillation on drag reduction. Soon after, Laadhari et al. (1994) confirmed experimentally the significant effect of spanwise oscillation. Recently, Choi et al. (1998) carried out precise measurements of channel turbulent flow with spanwise oscillation and discussed the mechanism of the drag reduction. They also found the same drag reduction effect in a circular pipe system. In addition to the effect of spanwise oscillation, Nakamura et al. (1998) indicated experimentally that wall oscillation in the normal wall direction in a rectangular channel had a drag-reducing effect like spanwise oscillation. Thus, oscillation of the channel wall does appear to have an effect on drag reduction. The flow configurations in the above studies are all related to rectangular or circular channels. More recently, Segawa et al. (2000) showed that a reduction of friction was observed by oscillating the bottom stationary disk in the rotating parallel disk system. It seems that the radial flow near the wall oscillation corresponds to the cross-flow in the channel.

During these three decades, extensive efforts have been made to clarify the ordered or coherent motion in wall turbulence. An important finding relating to the mechanism of turbulent friction is that turbulent skin friction is mainly generated by the so-called ejection of lower-speed clusters in the near-wall region into a higher stream region away from the wall (Kline et al. 1967) and sweep which is the in-rushing movement of high-speed fluid to the wall. This gives us some clues about controlling turbulent flow drag with regards to this movement. If we can produce a proper artificial disturbance, or control input, to cancel the aforementioned near-wall coherent structure, it may be possible to manage flow drag more efficiently. This strategy can be called a "controlled active method" as opposed to conventional active methods.

For the purpose of optimizing the design and drive condition of the actuator array, information on the spatial structure of the near-wall turbulence is necessary. Although LDV is applicable to the near-wall region, the measurement is limited only one point at a time. Thus we used particle image velocimetry (PIV), which has been recently recognized as a powerful tool for precise flow observation. Structure analyses of turbulent flow using PIV should lead to understanding turbulent flow and how to deduce turbulent frictional drags.

## 2. EXPERIMENTAL SETUP

Our experimental setup included a water channel and PIV and was basically the same as used by Li et al. (2000). Thus, in this section, the essential and specific points related to the present study will be described. The closed loop water channel system we used in this study is shown in Fig. 1. The channel is made of transparent acrylic plates to allow visualizing the flow by laser sheet. The channel was filled with bubble-free water and kept at temperature  $T = 30^\circ\text{C}$  by a cooling system. The test section was 40 mm high,  $H$ , 500 mm wide,  $W$ , and 6000 mm long,  $L$ . A series of experiments was carried out at Reynolds number 7500. The Reynolds number ( $Re$ ) is defined as:

$$Re = \frac{HU}{\nu},$$

where  $U$  is the mean velocity averaged over the duct cross-section and  $\nu$  is the kinematic viscosity of the water. In this experiment, the bulk mean velocity  $U$  equals 0.15 m/s. The flow control by means of the actuator array is carried out at the top or bottom wall of the channel at  $x = 3000$  mm downstream of the test section inlet. The flow becomes fully a developed turbulent flow around the measuring point.

According to the finding that turbulent friction is mainly caused by coherent motion near the wall, a strategy called a “controlled active method” focusing to coherent motion will be efficient to manipulate the turbulent friction. The sensor of coherent motion, actuator and control algorithm are essential components for establishing this controlled active method. The key issue in the development is an actuator driven by computer commands. Because the coherent motion spreads in space and moves over time, the actuator must have spatial distribution and sufficient temporal response. Other important factors are enough amplitude and durability in the fluid. Thus, in this study, a laminated piezo-ceramic element was selected as the material for the actuator array.

Figure 2 (a) shows a picture and schematic drawing of an actuator which consists of six laminated piezo-ceramic elements (Tokin Co., AE0203D16). Each element stretches  $17\ \mu\text{m}$  at 160 volts. Therefore the stroke of the actuators is more than  $100\ \mu\text{m}$  at 160 volts. The frequency response ranges from 0.1 to 1 kHz. A layout drawing of the actuator array is shown in Fig. 2 (b) and the array is composed of six laminated piezo-ceramic actuators. They can also oscillate from  $f_a = 1$  Hz to 1 kHz in the phase difference of 60 degrees to each other using six synchronized signal generators (NF Electric Instruments Co., NF1946). To control the coherent structure in a turbulent flow, the actuators are moved in various modes, for example the wavy mode shown in Fig. 3 (a).

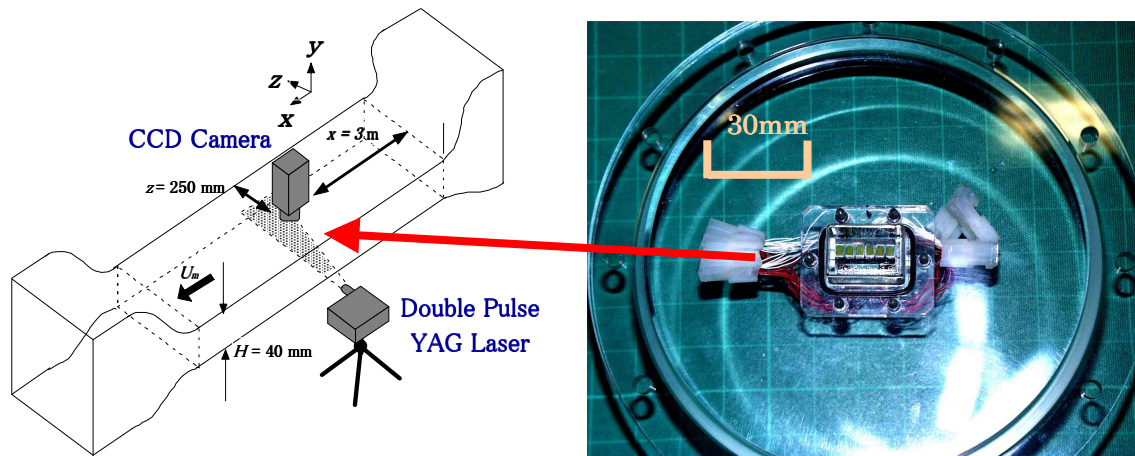


Figure 1 The closed-loop water channel system.

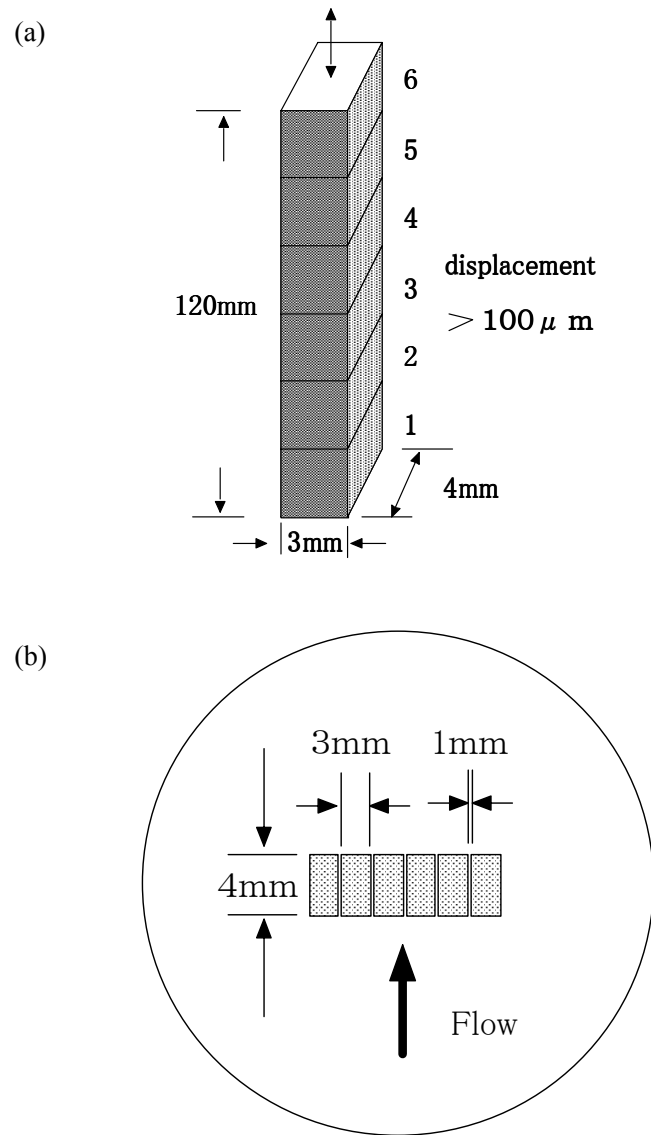


Figure 2 Picture and schematic drawing of an actuator which consists of six laminated piezo-ceramic elements.

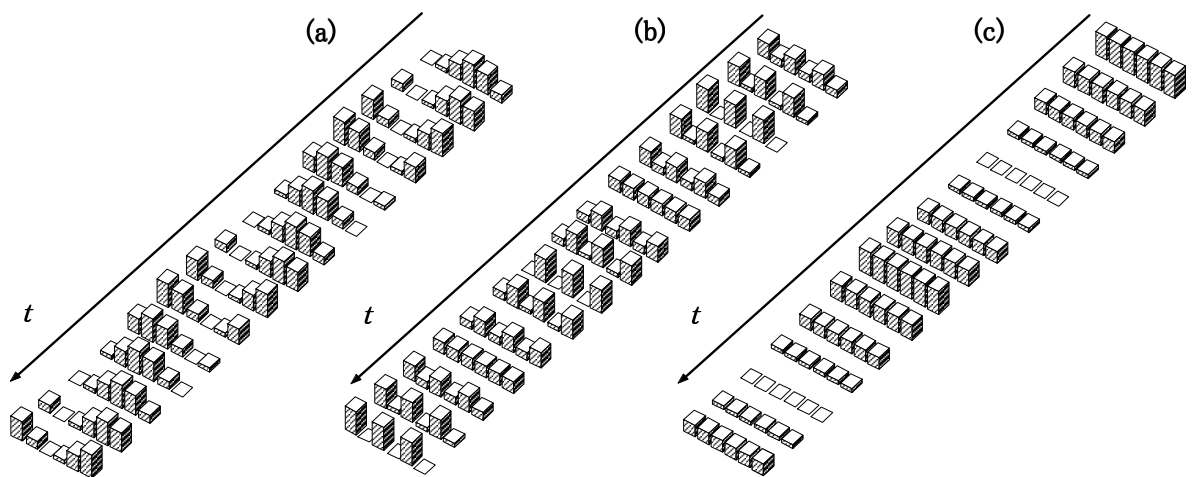


Figure 3 Schematic drawings of time evolution of surface shapes. (a) Mode I (Wavy), (b) Mode II (Alternative), and (c) Mode III (Gathering).

Here we introduce the length scale of the streak-like structure at  $y = 2$  mm from the upper or bottom wall. The friction velocity,  $u_\tau$ , is estimated as  $u_\tau = (\tau_w/\rho)^{1/2}$ , where  $\rho$  is the density of the fluid. Therefore  $u_\tau$  is roughly estimated at 0.01 m/s when using pure water at  $T = 30^\circ\text{C}$ . The most typical scale length  $\lambda$  of the streaks is known to be 100 times the viscous length scale,  $100 \nu/u_\tau$ . Thus a streak-like coherent structure of about 8 mm can be found at  $Re = 7500$ . We chose actuators with a width less than half of the streak's length scale ( $\lambda$ ) and arranged them at 4 mm intervals to control the fluid at  $1/2 \lambda$ . For example, it is possible to produce a disturbance in the spanwise direction by operating actuators in the wavy mode.

Regarding structure analyses, the areas where the vorticity and time evolutions of their low-speed ordered structures concentrate could be acquired within a 0.1 second interval. They will aid in our understanding of turbulent flow and establishment of a control method for it. The time scale on the burst was estimated to change flows and control bursts or horseshoe vortexes by active control. Luchik et al. (1987) reported on the averaged time between bursts,  $T_B$ . The non-dimensional time scale  $T$  of the bursting interval is defined as:

$$T = \frac{UT_B}{\frac{1}{2}H}.$$

For  $Re = 7500$ , we estimated that  $T = 0.6$  and  $T_B = 0.8$  second in our channel.  $T_B$  corresponds to the averaged occurring frequency of bursts,  $f_T = 1.25$  Hz. Thus the actuators can be oscillated up to 200 times higher than  $T_B$ .

The system setup for visualizing the flow is illustrated in Fig. 1. The actuator array is mounted on a circular plate set in the top wall of the channel at  $x = 3000$  mm downstream of the test section inlet. To visualize the near-wall flow, a pair of YAG laser sheets with the power of 25 mJ per pulse was set over the channel system. By changing the combinations of the cylindrical lenses, the laser sheet thickness can be modified in a range of 0.14 mm to 0.6 mm and a spread angle in the range of 4.3 deg to 13.3 deg. The images were photographed with a CCD camera at 1008 x 1018 resolution (PIVCAM 10-30, TSI Model 630046) and the velocity vectors were also analyzed by PIV software (TSI, Insight NT). The maximum frequency of the pulse was 15 Hz. Thus the time series of velocity and vorticity distributions were acquired as shown within a 0.1 second interval using the PIV system. Globular aluminum oxide ( $\text{Al}_2\text{O}_3$ ), which is 3 mm in diameter, was used as the seeding particle to obtain the images of the flow. By combining various lenses attached to the CCD camera, visualizations of the region from 2 x 2 mm to 40 x 40 mm were possible. The surface was covered with matte black film to prevent reflection of the laser light on the wall of the channel.

### 3. EXPERIMENTAL RESULTS and DISCUSSION

Figure 5 shows the velocity and vorticity distributions in the  $x$ - $y$  plane at  $Re = 7500$ . The laser was irradiated at  $z = 250$  mm, the midpoint between the side walls. In this paper, velocity and vorticity are described as color contour legends which are shown in Fig. 4. The low-speed structures were near the wall, though time averaged velocity and vorticity distributions did not have any characteristic spatial structure in this plane. These coherent structures are called a "horseshoe-like vortex". Rapid ejection of these low-speed structures from the plate is also well known as "bursts". Thus, the frictional drag was generated between the low- and high-speed structures. Therefore, it was considered that the vortex near the friction was likely to form in places near the top and bottom wall. In Fig. 5 we can see brilliant blue and red fields where the friction concentrates and the increase in vorticity was caused. Since bursts occur intermittently, it is useful to capture the time evolutions of velocity and vorticity to elucidate the bursting phenomena. Figure 5 also shows that the spatial structures were preserved for a short time and flow when riding on the main stream.

Figure 6 illustrates the signal of the velocity fluctuations in comparison with the displacement of an actuator. As the typical time scale  $T_B$  of the bursting interval, it was estimated that  $T_B$  equals 0.8 second using our channel.  $T_B$  corresponds to the averaged occurring frequency of bursts,  $f_B = 1.25$  Hz.

On the other hand, it is known that the frictional drag of turbulence is reduced by the compliant wall. Choi (2000) indicated that the effect appears when the wall's natural frequency synchronizes with not the bursting period but the bursting duration. Although the typical time scale of the bursting duration cannot be reported in our experiment, it should be much shorter than  $T_B$ . In this study, the frequencies of the actuators,  $f_a$ , were set at multiples of 1.25 Hz ( $= f_B$ ), for example at 6.25, 12.5, and 125 Hz, which correspond to 5  $f_B$ ,

$10 f_B$  and  $100 f_B$ . The actuators were oscillated in the phase difference of 60 degrees to each other and moved in the wavy modes as shown in Fig. 3 (a). Figure 9 also shows an overview chart of the structures generated by the wavy mode in the vicinity of the wall. Spotted fields, where the high- and low-speed streaks are mixed together, are formed. As a result, sine wave velocity fluctuations are caused in the spanwise direction. In Choi, et al.'s (1998) experiment using a rectangular channel, 20% of the frictional drag was reduced by spanwise oscillation of a channel wall. Our research is similar to their experiment with regards to inducing flow in the spanwise direction.

Figure 8 shows a photo of velocity distributions at  $y = 5$  mm from the bottom plate for Reynolds number,  $Re = 7500$ . The CCD camera was set at 15 mm upstream from the actuator array and images were acquired in 30 mm x 30 mm of the  $x$ - $z$  plane.  $y = 5$  mm corresponds to 50 times of well unit,  $y^+ = 50$  where mean velocity is about  $U = 0.15$  m/sec (Red zone in Fig. 8 (a)). The special scale length between the streaks was found to be about 10 mm, which is close to the empirical value  $\lambda$ , for  $Re = 7500$ . We can see in Fig. 8 (a) that fine spatial structures stay in the  $x$ - $z$  plane. On the other hand, Figs. 8 (b), (c), (d), (e) show velocity distributions using active control. The low-speed streaks are blurred for actuator frequencies over  $f_a = 12.5$  Hz as shown in Fig. 8 (d) and (e). Their shapes indicate that the spatial structures can be made to disappear by an active control. The critical frequency,  $f_a = 12.5$  Hz at which the coherent structures were destroyed, seems to correspond to  $10 f_B$ . At present, we are studying whether the typical time scale of the bursting duration is the same order as  $1/10$  of  $T_B (=1/10f_B)$ . Here we consider how a disturbance of 0.1mm ejected from the stationary plate by the actuator grows at 15 mm upstream in the  $x$  direction. The growth size  $\delta$  of disturbance is introduced as:

$$\delta \approx 5 \sqrt{\frac{xV}{U_f}},$$

where  $U_f$  is the free stream velocity and 0.18 m/sec in this experiment. Therefore the length scale of growth is estimated as  $\delta=4.5$  mm for  $Re=7500$ . As  $\delta$  comparable to the length scale of streaks, disturbances can interact with streaks sufficiently.

We consider it not to be nontrivial that the low-speed streaks disappear by such periodic inputs because the motions of turbulent structures are not stationary and do not always synchronize with the periodic motion of disturbances by the actuators. In one case, an actuator can move by synchronizing its phase with the coherent structures and with the opposite phase in the other case. The former will activate the systematic structures, and the latter inhibit them, if the phenomenon near wall responses are linear. Therefore it seems that these phenomena are nonlinear and the disturbances always diffuse the coherent structures.

It is also well known that some artificial streaks with regular intervals on the wall, called riblets, can reduce the flow drag (For example as reported by Walsh et al. (1984)). It is considered that a similar nonlinear phenomenon occurs near the riblets because the convexes of the riblets don't always agree with the positions where low-speed streaks are seen. It is also same regarding the concaves. Restricting the motion of the streaks and tidying them up along the riblets seems the reason why the riblets have the effect of reducing drag. Our control method, enumerating artificially, is similar to the riblets but seems to be smart to flexibly correspond to various flow conditions. Endo et al. (2000) carried out direct numerical simulations of an active flow control using arrayed sensors and an actuator unit. The actuator, which they proposed in their simulation, can deform and create disturbances to cancel the vorticities of streaks in the vicinity of the wall. Using their method, it was found that streak structures near the wall could be ordered along the flow direction and could decrease the frictional drag as well as riblets.

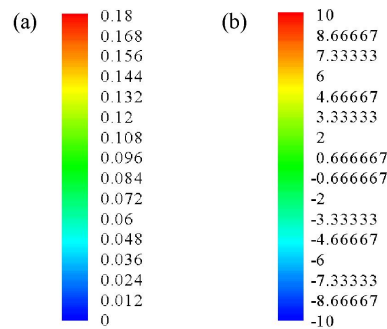


Figure 4 (a) Contour legend of velocity. (b) Contour legend of vorticity.

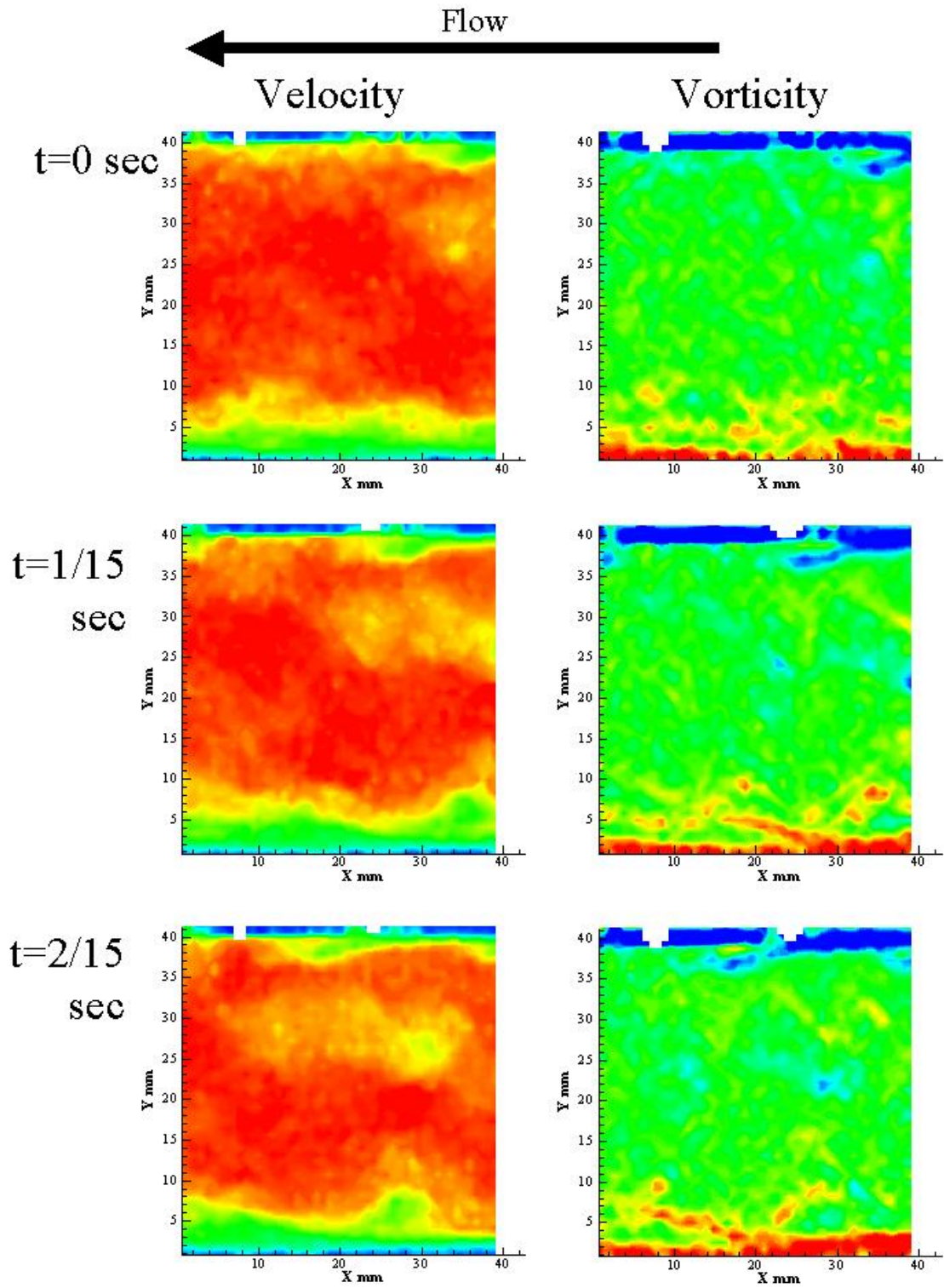


Figure 5 Time series of velocity and vorticity distribution in  $x$ - $y$  plane.  $Re = 7500$ . It flows from right to left. (a) Velocity. (b) Vorticity.



## Bursting Duration

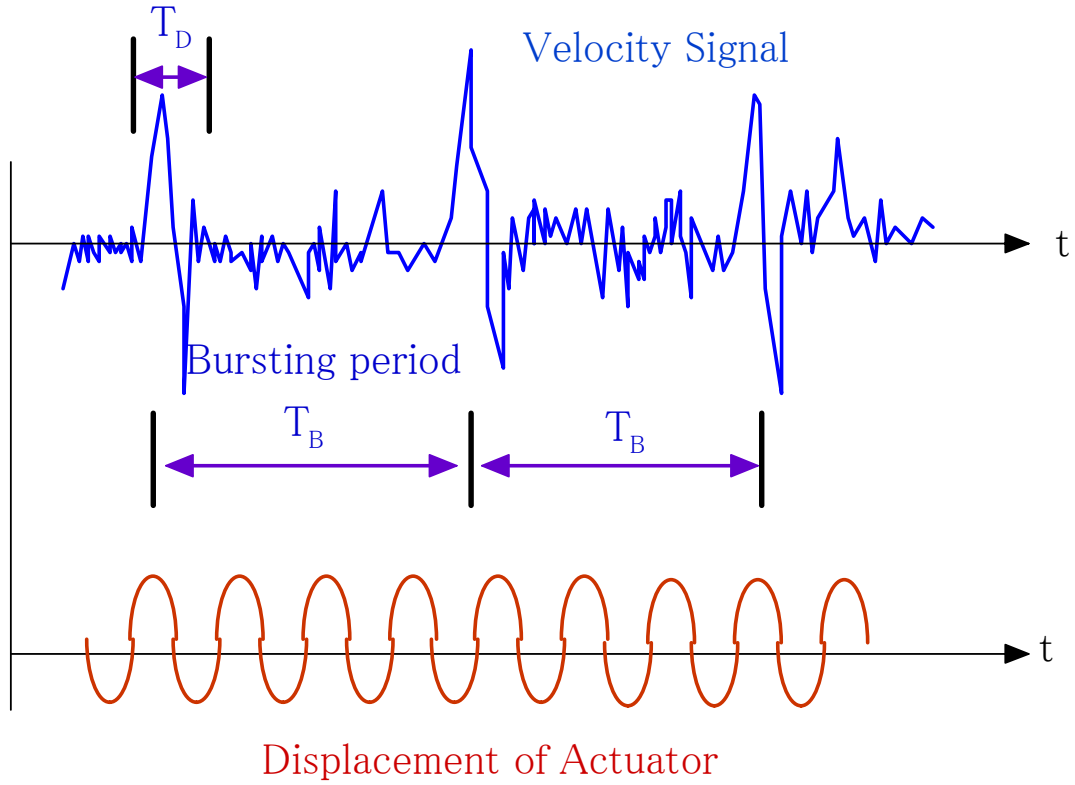


Figure 6 Schematic drawing of velocity fluctuation near the wall in comparison with displacement of actuator.

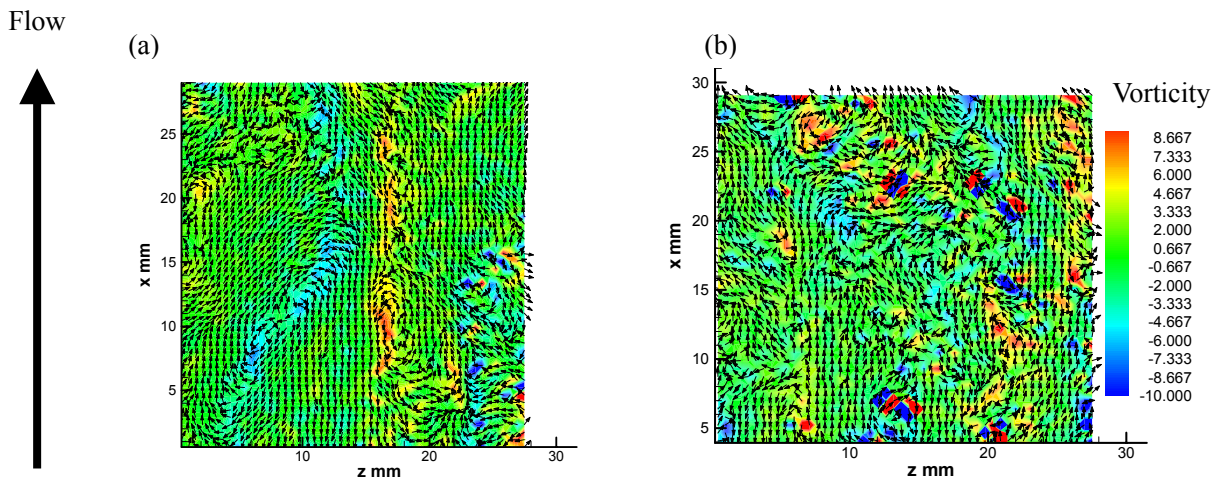
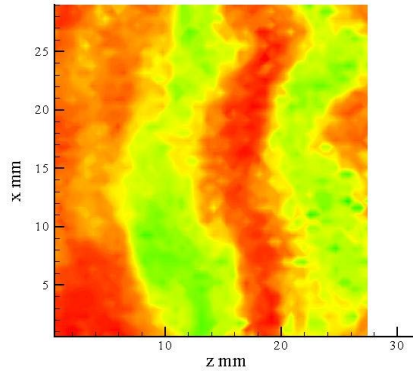
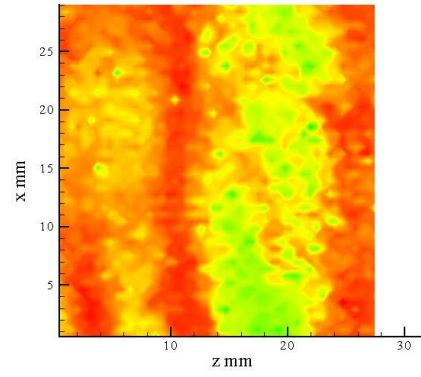


Figure 7 Instantaneous velocity (vectors) and vorticity (color contours) distributions of  $x$ - $z$  plane at  $y = 5$  mm to ( $y^+ = 50$ ) visualized by PIV. (a) No control. (b)  $f_a = 125$  Hz. Actuator array is set 15 mm upstream. Velocities corresponding to mean value of visualized area have been subtracted from all vectors.

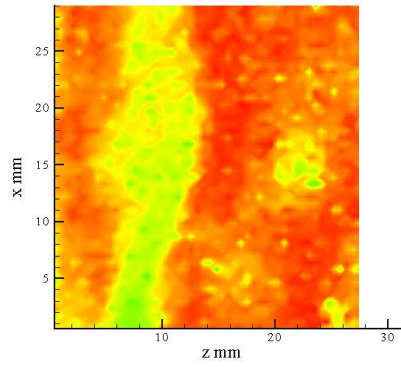
(a)



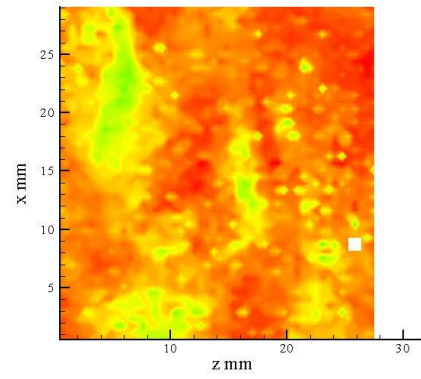
(b)



(c)



(d)



(e)

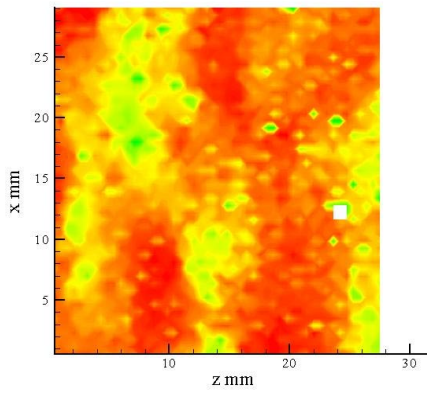


Figure 8 Typical velocity distribution in  $x$ - $z$  plane,  $Re = 7500$ .



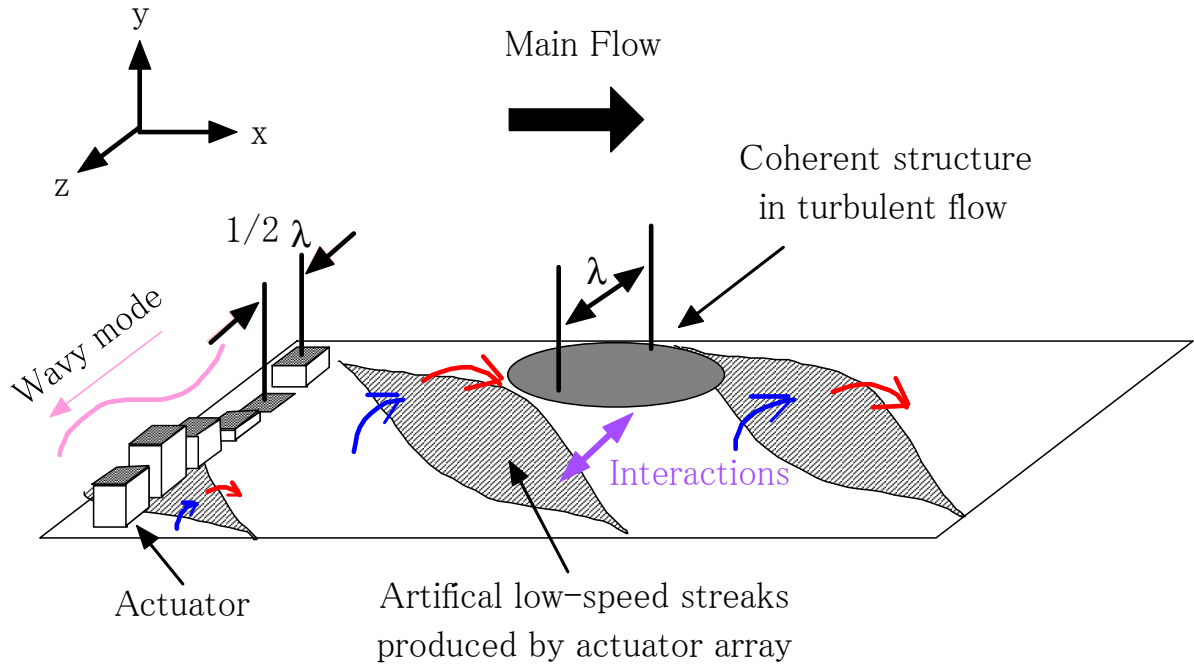


Figure 9 Schematic illustration of streaks.

The velocity of the progressive wave generated by the wavy mode of the actuator array is  $U_s = 0.30$  m/s at  $f_a = 12.5$  Hz in spanwise direction. As the free-stream velocity is  $U_f = 0.18$  m/sec, the ratio of the spanwise velocity to the free stream velocity is  $U_s/U_f = 1.7$ . On the other hand, the amplitude of the spanwise velocity component in Choi et al.'s experiment was estimated to be  $U_s = 1.5$  m/sec at maximum as against  $U_f = 2.5$  m/sec. Thus the ratio of the spanwise velocity to the free-stream velocity is  $U_s/U_f = 0.6$ . Because  $U_s/U_f$  is much larger than that of Choi et al. (1992), frictional drag can be reduced in our experiment though we have not observed it yet.

In the wavy mode, ordered structures in the vicinity of the wall may be destroyed and the frictional drag can increase at frequencies over  $f_a = 12.5$  Hz as shown in Fig. 8. Therefore we have carried out our experiments in other modes, "Alternative mode" or "Gathering mode" as shown in Fig. 3. These modes also can create spanwise perturbations on the streaks. Although the effect of drag control in these modes have not been found at present, they may lead to turbulent drag reduction if low-speed streaks can be arranged in the flow direction. We are also thinking of using their actuators as a tool for heat and mass transfer enhancements.

We wish to acknowledge that Mr. T. Ohki of Nippon University prepared the figures. The authors would like to express their sincere thanks to Professors N. Kasagi and Y. Suzuki of the University of Tokyo, Drs. Y. Tsutsui and A. Yabe of the Mechanical Engineering Laboratory and Dr. K.-S. Choi of the University of Nottingham for their kind advice and stimulating discussions. This research was carried out at the Center for Smart Control of Turbulence funded by MECSST of Japan.

#### 4. CONCLUSIONS

The coherent structures of turbulent flow in a channel flow for  $Re = 7500$  were analyzed using PIV. The main results are as follows:

- (1) The horseshoe-like structures and bursts occurring near the wall were visualized.
- (2) The rapid separations of bursts from the wall caused local concentrations of vorticity and their spatial structures were preserved for a short time and flow while riding on the main stream.
- (3) The regularity of the velocity distribution tended to decrease at actuator frequencies over  $f_a = 12.5$  Hz, compared to when it was not controlled.

- (4) The length scale of the growth of disturbances ejected from the wall caused by the actuators was estimated as  $d = 4.5$  mm for  $Re = 7500$ . These disturbances can sufficiently interact with the streaks and the coherent structures can be made to disappear using an active control.

With these conditions, it was proven that the coherent structures in the vicinity of the wall can be made to interact with the disturbance using an actuator array, and an experiment for active control of turbulent flow was described in this study.

## REFERENCES

1. Choi, K.-S., DeBisschop, J.-R. and Clayton, B. R. (1998). "Turbulent boundary-layer control by means of spanwise-wall oscillation", *AIAA Journal* **36**, pp. 1157-1163.
2. Choi, K.-S. and Graham, M. (1998). "Drag reduction of turbulent pipe flows by circular-wall oscillation", *Phys. Fluids* **10**, pp. 7-9.
3. Choi, K.-S. (2000). ; "Turbulent drag-reduction mechanisms: strategies for turbulence management", Springer-Verlag Lecture Notes, to be published.
4. Choi, H., Moin, P. and Kim, J. (1994). "Active turbulence control for drag reduction in wall-bounded flows", *Journal of Fluid Mechanics* **262**, pp. 75-110.
5. Endo, T., Kasagi, N. and Suzuki, U. (2000). "Control of wall shear turbulence with arrayed micro sensor/actuator units" *Proc. 4<sup>th</sup> JSME-KSME Thermal Engineering Conference*, vol. 3, pp. 493-498.
6. Hama, F. R., Long, J. D. and Hegarty, J. C. (1957). "On transition from laminar to turbulent flow", *Journal of Applied Physics* **28**, pp. 388-394.
7. Jung, W. J., Mangiavacchi, N. and Akhavan, R. (1992). "Suppression of turbulence in wall-bounded flows by high frequency spanwise oscillations", *Physics of Fluids* **A4**, pp. 1605-1607.
8. Kimura, M., Tung, S., Lew, J., Ho, C.-M., Jiang, F. and Tai, Y.-C. (1999). "Measurement of wall shear stress of a turbulent boundary layer using a micro-shear-stress imaging chip", *Fluid Dynamic Research* **24**, pp. 329-342.
9. Kline, S. J., Reynolds, W. C., Schraub, F. A. and Runstadler, P. W. (1967). "The structure of turbulent boundary layers", *Journal of Fluid Mechanics* **30**, pp. 741-773.
10. Kumar, S. M., Reynolds, W. C. and Kenny, T. W. (1999). "MEMS based transducers for boundary layer control", *Proc. 12th IEEE International Conference on Micro Electro Mechanical Systems*, pp. 135-140.
11. Laadhari, F., Skandaji, L. and Morel, R. (1994). "Turbulence reduction in a boundary layer by a local spanwise oscillating surface", *Physics of Fluids* **A6**, pp. 3218-3220.
12. Li, P.W., Kawaguchi, Y., Segawa, T. and Yabe, A. (2000). "Turbulent Structure in a Drag-reducing Channel Flow with Surfactant Additives", *Proc. 10th International Symposium on Applications of Laser Techniques to Fluid Mechanics*, 27\_5, pp. 1-12.
13. Luchik, T. S. and Tiederman, W. G. (1987). "Timescale and structure of ejections and bursts in turbulent channel flows", *Journal of Fluid Mechanics* **174**, pp. 529-552.
14. Nakamura, M., Sakai, E., Igarashi, O. and Masaoka S. (1998). "Experimental study on the pressure distribution of a flow through a two-dimensional channel with oscillating wall", *Nagare* **17**, 444 (in Japanese).
15. Segawa, T., Yoshida, H., Kikushima, Y. and Tsutsui, Y. (2000). "An attempt of active flow control in rotating disk system", *Proc. ASME Pressure Vessels and Piping Conference, Emerging Technologies in Fluids, Structures, and Fluid/Structure Interactions Vol. 2*, pp. 133-118.
16. Stuart, A., Jacobson, A. and Reynolds C. W. (1998). "Active control of streamwise vortices and streaks in boundary layers", *Journal of Fluid Mechanics* **360**, pp. 179-211.
17. Walsh, M. J. and Lindemann, A. M. (1984). "Optimization and application of riblets for turbulent drag reduction", *AIAA paper* 84-0347.
18. Zhou, J., Meinhart, D. C., Balachandar, S., and Adrian, J. R. (1997). "Formation of coherent hairpin packets in wall turbulence", edited by Panton, L. R., *Self-sustaining Mechanics of Wall Turbulence*, Computational Mechanics publications, Southampton, pp. 109-134.